Electronic Supplementary Material (ESI) for Lab on a Chip.

Supplementary Information

Microfluidic arrays of dermal spheroids: a screening platform for active ingredients of skincare products

*Zhengkun Chen[1], Sina Kheiri[2], Albert Gevorkian[1], Edmond W.K. Young[2], Valerie Andre[3], Ted Deisenroth[4], Eugenia Kumacheva[1,5,6] **

[1] Department of Chemistry, University of Toronto, 80 Saint George Street, Toronto, Ontario, Canada, M5S 3H6

[2] Department of Mechanical and Industrial Engineering, University of Toronto, Toronto, Ontario, 5 King's College Road, Toronto, Ontario, Canada, M5S 3G8

[3] BASF Beauty Care Solutions France S.A.S., 32, rue Saint Jean de Dieu, Lyon, France, 69007

[4] BASF Advanced Formulation Research North America, 500 White Plains Road, Tarrytown, New York, USA, 10591

[5] Department of Chemical Engineering and Applied Chemistry, University of Toronto, 200 College Street, Toronto, Ontario, Canada, M5S 3E5

[6] Institute of Biomaterials and Biomedical Engineering, University of Toronto, 4 Taddle Creek Road, Toronto, Ontario, Canada, M5S 3G9

1. Design of the microfluidic device

Figure S1A illustrates the allocation of 12 quadruplets with cylinder-shape microwells with diameter of 100 µm, placed in a 75 mm × 50 mm microfluidic (MF) device. A quadruplet with 100 µm-diameter wells takes up an area around 1.5 mm × 23 mm. Figure S1B shows the dimensions of a quadruplet with 100 µm-diameter wells (which have the height of 127 µm), while the supplying channel has the width of 67 µm and height of 27 µm. These dimensions are all increased three-fold in the quadruplet with 300 µm-diameter microwells: the microwell are 300 µm in diameter and 360 µm in height, while the supplying channel is 200 µm wide and 80 µm high.

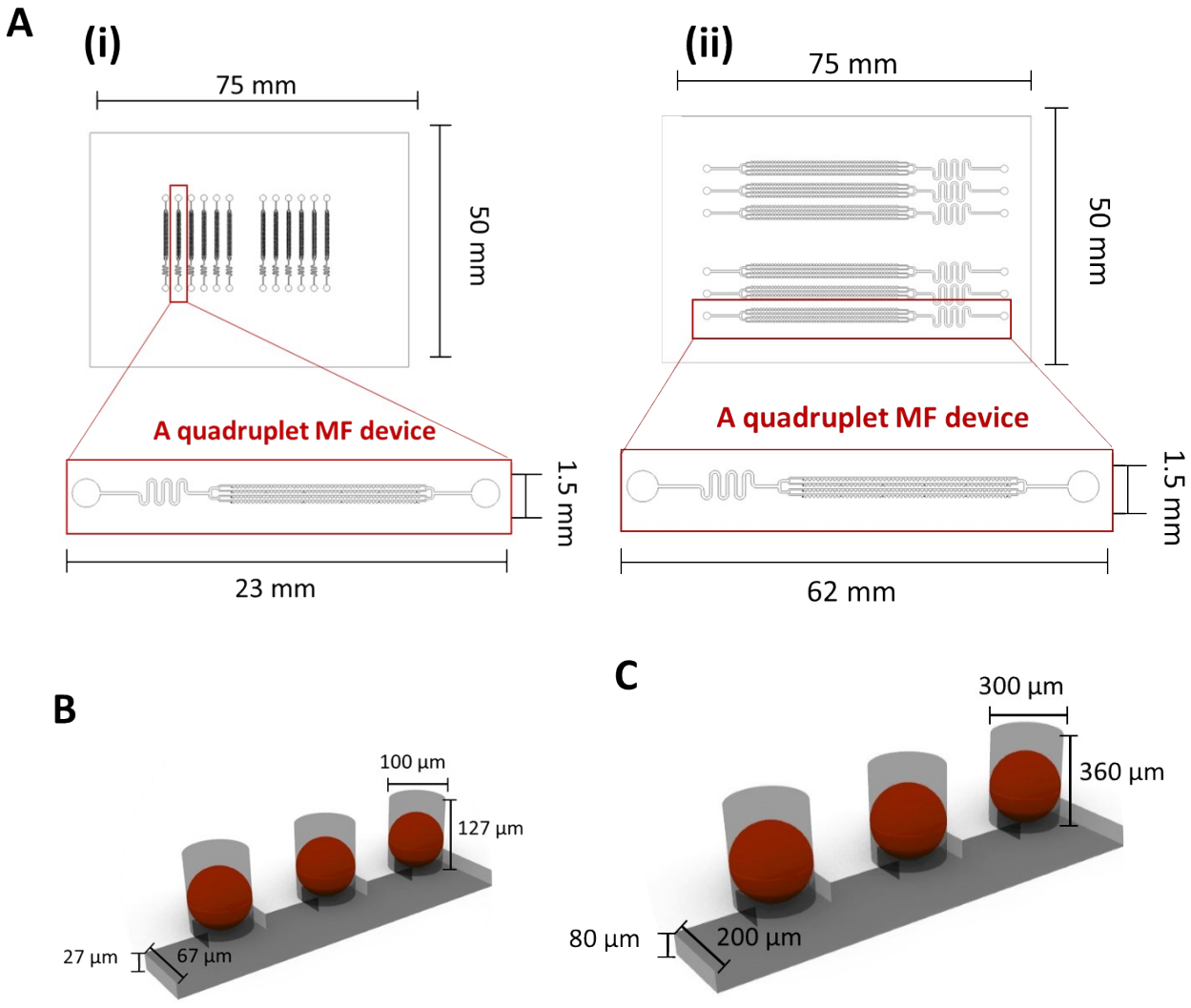

Figure S1. Characteristic dimensions of a dermal spheroids-on-a-chip MF platform. (A) Schematic of a MF device containing 12 quadruplets with microwell diameter of (i) 100 µm and (ii) 300 µm. (B) 3D rendered schematic of a MF array with 100 µm-diameter microwells. (C) 3D rendered schematic of a MF array of 300 µm-diameter microwells.

2. Formation and maintenance of DFSs in a MF platform with 300 µm-diameter microwells

Figure S2 shows the success rate in the formation of cell-laden droplets and the survival rate of the DFSs in the 300 µm-diameter microwells in experiments conducted at different cell densities. At high cell density (corresponding to 7000-10000 cells/DFS), a high success rate was obtained. Each microwell was filled with cell-laden droplets of uniform size and density (Figure S1A). The success rate reduced with a decrease in celldensity. At 500 cells/DFS, a fraction of microwells was filled with ill-defined cell-laden droplets or remained empty (Figure S1A). On Day 5, the majority of the DFSs that were formed at a high cell density (7000-1000 cells/DFS) remained inside microwells (Figure S1C). A low survival rate was observed for the DFSs formed at low density (500-4000 cells/DFS), that is, most of the DFSs were washed away.

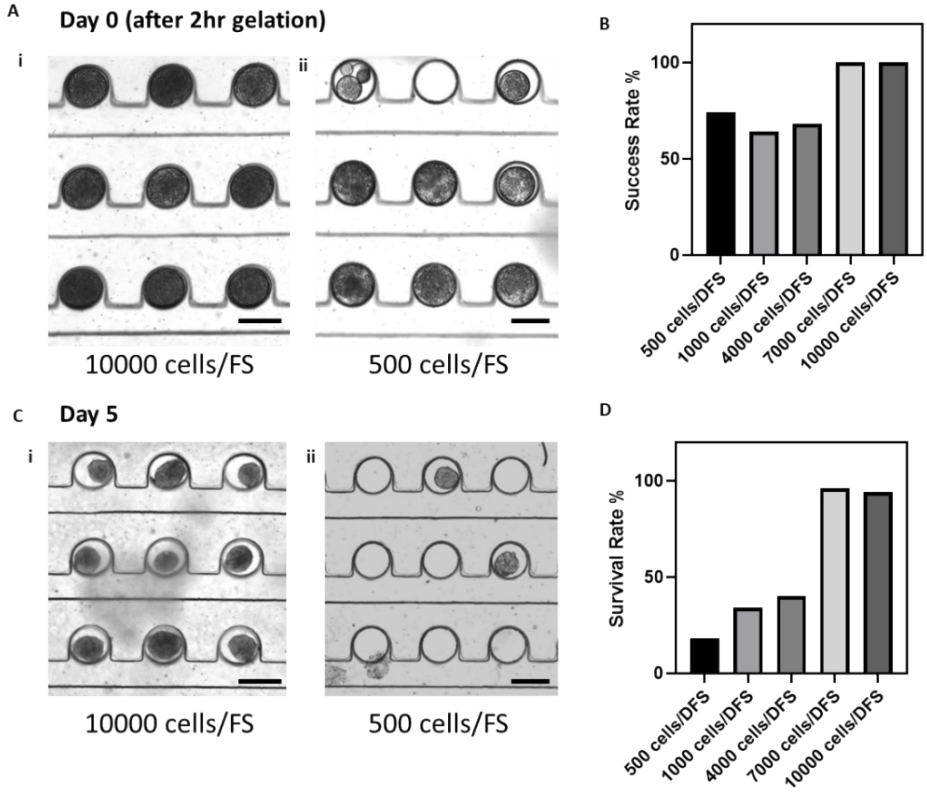

Figure S2. Formation and maintenance of DFSs in a MF platform with 300 µm-diameter microwells. (A) Representative brightfield images of cell-laden droplets formed on Day 0 from the cell suspensions with different cell densities. (B) The success rate on Day 0. (C) Representative brightfield images of cell-laden microgels formed from the cell suspension with different cell densities and maintained on Day 5. (D) Survival rate of cell-laden microgels as in (C) on Day 5. The scale bar is 300 µm. N =1.

3. Contraction of DFSs over time

Figure S3 shows the change in DFS dimensions over 5-day culture in the MF quadruplet device. The average DFS dimensions were measured from its area by analyzing brightfield images. The size of the DFSs significantly decreased from Day 1 to Day 3. The decrease in the DFS size stopped on Day 3, that is,

no significant change in the DFSs' area was observed on Days 3-5. Thus the DFSs reached an invariant size on Day 3. Notably, vitamin C did not influenece the size of the DFSs.

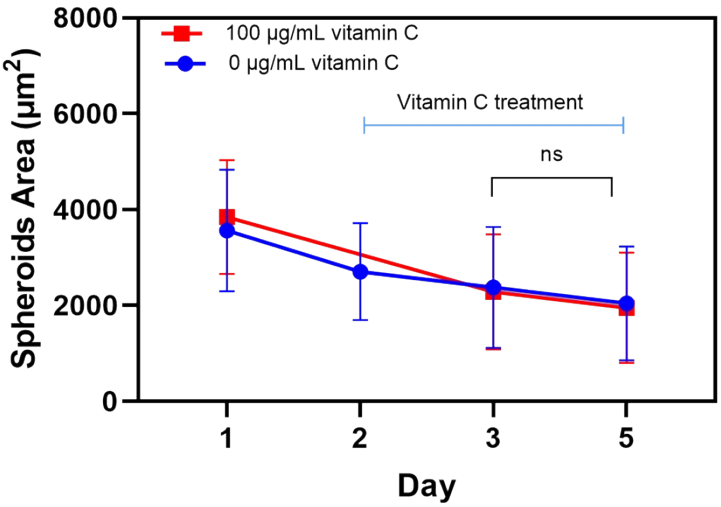

Figure S3. DFSs area over 5 days of on-chip culture with or without vitamin C treatment. Two-way ANOVA Tuckey's post hoc $^{ns}p>0.05$.

4. Table S1. Summary of the modelling details

Software and solver	
Geometry software	COMSOL Multiphysics 5.6
Physics types (COMSOL)	Laminar Flow (*Spf*) and Transport of Diluted species (tds)
Study types (Transient or Steady)	Stationary
Solver	Fully Coupled (Direct)
Mesh	
Number of elements	820 000 - 1650 000
Mesh Type	Adaptive and calibrated for fluid dynamics
Flow properties	
Material	Water
Viscosity	0.001 Pa s
Density	1000 kg/m^3

Porous matrix properties

Material	Hydrogel (manually defined)
Porosity	0.5
Permeability	8×10^{-11} cm^2
Diffusion coefficient of molecule	1.78×10^{-10} m^2/s

Boundary conditions

Inlets flow condition	Fully developed Flow (Pressure= 5 Pa)
Inlets transport condition	Constant concentration (20, 50, 75 and 100 µg/mL)
Outlets condition	Constant pressure (0 Pa, gauge)
Walls	No slip condition & no Flux

The following governing partial differential equations were implemented in our COMSOL model

$$\rho(u \cdot \nabla)u = \nabla \cdot [-pl + K] + F \quad (1)$$

$$\rho \nabla \cdot u = 0 \quad (2)$$

$$\nabla \cdot J_i + u \cdot \nabla c_i = R_i \quad (3)$$

$$J_i = -D_i \nabla c_i \quad (4)$$

where ρ is the fluid density, u is the velocity vector, p is the pressure, F is the volume force vector, J is the diffusive mass flux, R is the reaction rate expression for species, D is the diffusion coefficient, and c is the concentration of species. Equation (1) represents the Navier-Stokes equations; Equation (2) represents the continuity equation; Equation (3) represents mass transport of species ci; and Equation (4) represents Fick's first law of diffusion.

The solute penetration into spheroids on a MF chip depends on pressure gradients in microchannel, spheroid permeability, drug diffusivity, and concentration of the solute in the media. A 3D CFD model was developed to examine the effect of these characteristics on solute transport in DFSs.

In the first step, the pressure and velocity gradient in the MF device were modelled using the laminar flow module in COMSOL Multiphysics 5.6 software. Table S1 summarizes the initial and boundary conditions used in the simulations. Fig. S4 shows the pressure drop along the microchannel. To model vitamin C transport, the results of laminar fluid flow was coupled with the transport of the diluted solute module in COMSOL. To study and compare advection and diffusion fluxes in spheroids under different concentrations of vitamin C, the spheroid inside the microwell was modelled as a porous matrix domain (Fig. S4 insert).

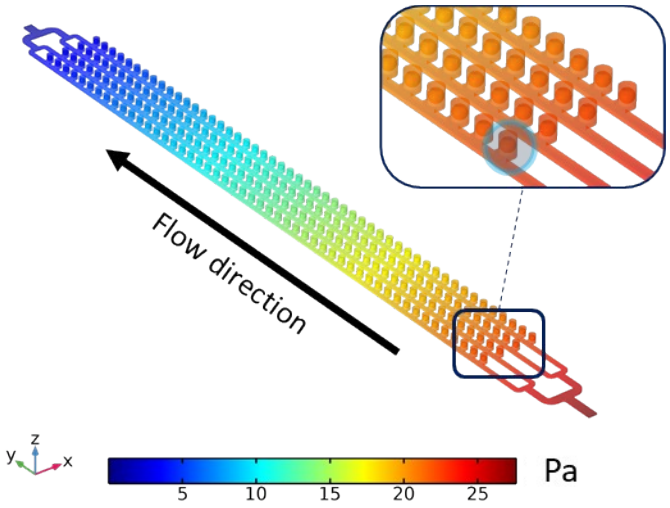

Figure S4. Pressure gradient contours in the full-device of the quadruplet MF arrays from CFD simulations.

5. Fluorescence intensity of cell nuclei in DFSs

Figure S4 shows the measured fluorescence intensity of nuclei in the DFSs on Day 5 with 0 μg/mL and 100 μg/mL Vitamin C. No significant difference was observed between two groups.

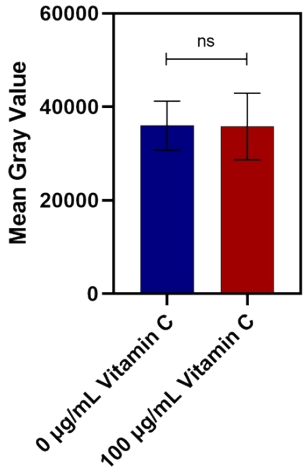

Figure S5. Fluorescence intensity of nuclei in the DFSs on Day 5 with 0 μg/mL and 100 μg/mL Vitamin C. t-test: $^{ns}p>0.05$.

6. Table S2. Antibodies used for immunofluorescence staining

Antigen	Primary Antibody	Secondary Antibody
E-cadherin	Alexa Fluor 488 E-Cadherin rabbit monoclonal antibody (1:800 dilution, Cell Signaling Technology™)	
F-actin	165 nM/mL Alexa Fluor 568 Phalloidin	

	(Life technologies™)	
Collagen Type I	Rabbit anti-human collagen type I polyclonal antibody (1:250 dilution, Invitrogen™)	Goat anti-rabbit IgG Alexa Fluor 546 (1:500 dilution, Invitrogen™)
Fibronectin	Mouse anti-human fibronectin monoclonal antibody (1:100 dilution, Invitrogen™)	Goat anti-mouse IgG Alexa Fluor 488 (1:400 dilution, Invitrogen™)
Nuclei	0.5 ng/mL Hoechst 33342 solution (Invitrogen™)	